Preparation and Electrical Properties of Ultrafine Ga_2O_3 Nanowires

Yang Huang,[†] Shuanglin Yue,[†] Zhongli Wang,[†] Qiang Wang,[†] Chengying Shi,[†] Z. Xu,[†] X. D. Bai,[†] Chengcun Tang,[‡] and Changzhi Gu*[,†]

Beijing National Laboratory for Condensed Matter Physics, Institute of Physics, Chinese Academy of Sciences, Beijing 100080, P. R. China, and Department of Physics, Central China Normal University, Wuhan 430079, P. R. China

Received: October 12, 2005; In Final Form: November 10, 2005

Uniform and well-crystallized β-Ga_2O_3 nanowires are prepared by reacting metal Ga with water vapor based on the vapor−liquid−solid (VLS) mechanism. Electron microscopy studies show that the nanowires have diameters ranging from 10 to 40 nm and lengths up to tens of micrometers. The contact properties of individual Ga_2O_3 nanowires with Pt or Au/Ti electrodes are studied, respectively, finding that Pt can form Schottky-barrier junctions and Au/Ti is advantageous to fabricate ohmic contacts with individual Ga_2O_3 nanowires. In ambient air, the conductivity of the Ga_2O_3 nanowires is about 1 $(\Omega\cdot m)^{-1}$, while with adsorption of NH_3 (or NO_2) molecules, the conductivity can increase (or decrease) dramatically at room temperature. The as-grown Ga_2O_3 nanowires have the properties of an *n*-type semiconductor.

1. Introduction

One-dimensional nanoscale materials such as nanotubes, nanowires, and nanobelts have attracted much attention because of their importance in understanding fundamental physical concepts and potential applications in building blocks for electronic and optical nanodevices.[1,2] Recently, the local electrical and optical properties of individual nanowires or nanotubes have been extensively studied to understand the intrinsic physical properties of these nanomaterials. Some interesting phenomena have been observed in oxide systems; for example, enhanced sensitivity was obtained in individual SnO_2- and ZnO-nanowire-based transistors.[3,4]

Intrinsic monoclinic gallium oxide (β-Ga_2O_3) is an important wide band gap material (band gap energy of 4.9 eV) and has been widely used as the insulating oxide layers for gallium-based electric devices. Prepared under reducing conditions, gallium oxide becomes an *n*-type semiconductor due to oxygen vacancies. The vacancies can act as shallow donors with ionization energy $E_d = 0.03-0.04$ eV.[5] Previous studies indicated that the *n*-type semiconductor exhibits remarkable conduction and luminescence characteristics[5,6] and can be used as optoelectronic devices, spin tunneling junctions, and high-temperature gas sensors.[7,8] So far, Ga_2O_3 nanowires and nanobelts have been synthesized by several methods, such as physical evaporation,[9] silica-assisted catalytic growth,[10] laser ablation,[11] carbon thermal reduction,[12] and so on. However, little research has been done on the electrical properties of an individual Ga_2O_3 nanowire.[13]

In this paper, we proposed a novel way to synthesize Ga_2O_3 nanowires with a uniform diameter by reacting metal Ga with water vapor based on the vapor−liquid−solid (VLS) mechanism. The water vapor enhanced the growth rate of the nanowires, which is a cheap, clean, and safe assistance compared with the Si, C, or H_2 used in the previous method. The electrical properties of an individual Ga_2O_3 nanowire were studied by preparing contact electrodes with Pt and Au/Ti, respectively. The adsorption properties of Ga_2O_3 nanowires in various ambient gases were studied.

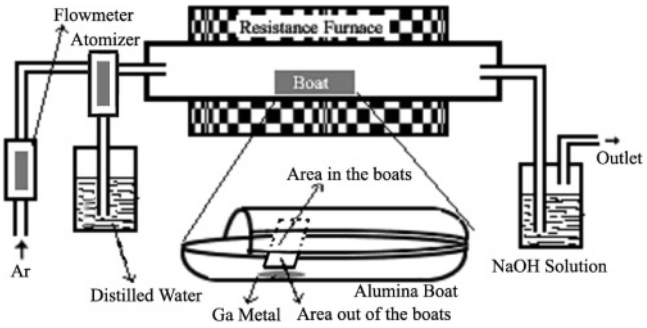

Figure 1. Illustration of the experimental setup. The atomizer is connected to a glass flask containing the distilled water.

2. Experimental Section

A silicon substrate (10 mm × 10 mm) was first cleaned in an ultrasonic bath, using acetone, for about 1 h. Then a 20-nm layer of Au was deposited on the substrate by using the DC sputtering method. Then Ga metal particles of about 500 mg were put into an alumina boat, and the Au-coated Si substrate was put onto the alumina boat, with the Au layer turned toward the gallium source below, separated by ∼5 mm. The substrate was further secured by an inverted boat with a section cut away, as shown in Figure 1. This setup was helpful to us in understanding the growth mechanism of the short nanowires. A conventional tube furnace with an atomizer system containing the distilled water was used in our experiment. The atomizer generates homogeneous water vapor during the reaction. After the alumina boats were transferred into the quartz tube mounted in the furnace, the reaction system was first flushed with argon gas of 600 sccm for 10 min to eliminate the air and then was rapidly heated to 900 °C within 20 min. The flow of argon gas was also adjusted to 200 sccm simultaneously. At the reaction

* To whom correspondence should be addressed: E-mail: czgu@aphy.iphy.ac.cn.
[†] Chinese Academy of Sciences.
[‡] Central China Normal University.

10.1021/jp055844p CCC: $33.50
Published on Web 12/13/2005

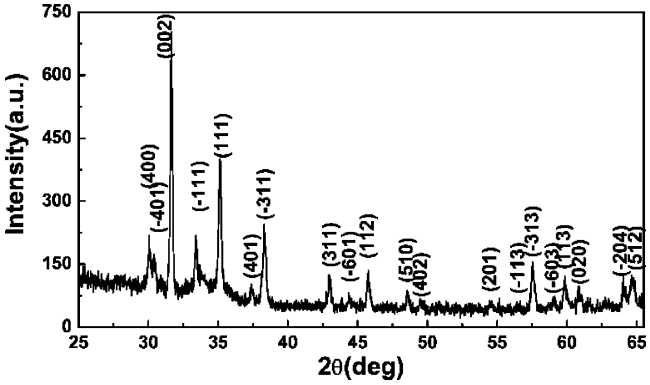

Figure 2. X-ray diffraction pattern for the white product on the substrate.

temperature, distilled water was atomized and reacted with the metal Ga at the central hot zone. After the reaction proceeded for 20 min, the atomization operation was stopped, and the furnace was cooled to room temperature with the argon flow.

After the reaction, a homogeneous white film was observed on the substrate within the boats, and no visible product was observed on substrate extending outside of the boats. The product was characterized with X-ray diffraction (XRD, D/MAX-rB, Cu Kα radiation), a field-emission scanning electron microscope (SEM, JEM-6700F, JEOL) operated at an accelerating voltage of 10 kV, and a high-resolution transmission electron microscope (TEM, JEOL-3100F) equipped with an energy-dispersive X-ray (EDX) analysis system.

To measure the electrical properties of an individual Ga_2O_3 nanowire, as-grown Ga_2O_3 nanowires were first ultrasonically dispersed in ethanol, and then the ethanol dispersions were dried onto a silicon wafer covered with a thermally grown SiO_2 layer of 500 nm. Isolated nanowires were selected and located in a focused ion-beam (FIB) system with SEM capability (Dual-Beam 235 FIB system from FEI Company). Platinum electrodes, 1.0-μm wide and 0.8-μm thick, were directly written on an appropriate nanowire by using a 30-keV, 30-pA Ga^+ FIB. The thermal annealing was performed in a flowing Ar atmosphere at 400 °C for 10 min by using the tube furnace. Au/Ti electrodes were fabricated by electron-beam lithography (EBL). In brief, the contacts were first designed by electron-beam lithography (with a Raith 150), and then a 30-nm Ti adhesive layer covered by a 50-nm Au was sputtered onto the sample by using a radio frequency (RF) magnetron sputtering system followed by a lift-off process. Electrical connection between the electrodes and the sample holder was made with an ultrasonic wire bonder. The devices were transferred in a small shield chamber with electrical feed-through, and the electrical measurements were carried out at room temperature. The contact properties between electrodes and Ga_2O_3 nanowires were studied directly in air. For the gas sensitivity study, the conductance of the nanowires was monitored while flowing dry air-diluted NH_3 and NO_2, respectively.

3. Results and Discussion

Figure 2 shows the XRD pattern of the white product on the substrate. The diffraction peaks can be indexed to a monoclinic structure of gallium oxide with cell constants of $a = 1.223$ nm, $b = 0.304$ nm, $c = 0.580$ nm, and $\beta = 103.7°$, in agreement with the standard diffraction data (JCPDS 76-573). We have noticed that the relative intensities of the diffraction peak exhibit a considerable difference between the present pattern and the standard pattern of bulk β-Ga_2O_3. For example, the ideal

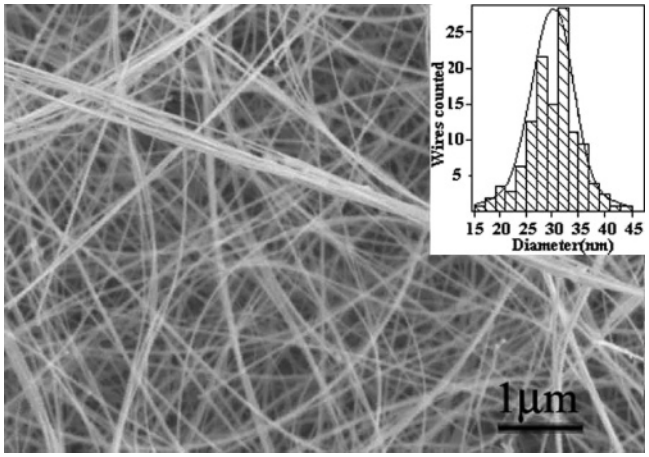

Figure 3. Scanning electron microscopy images taken from the substrate in the boats showing abundant Ga_2O_3 nanowires with a high aspect ratio. Inset shows the statistic histogram of the nanowire diameters distribution, indicating that the average diameter of the nanowires is 30 ± 5 nm.

intensity ratio between (111) and (−311) is less than 0.9, whereas the measured ratio in this study is larger than 1.6. This phenomenon may be attributed to preferential growth of one-dimensional structure.[14]

The typical SEM images taken of the homogeneous white layer on the substrate, as shown in Figure 3, reveal that abundant uniform nanowires with a high aspect ratio lie twisted together on the substrate. Although there are some nanowires with larger diameters, the histogram of the nanowire diameter distribution plotted in the inset of Figure 3 clearly indicates that the Ga_2O_3 nanowires have a comparatively centralized diameter distribution and the average diameter of the nanowires is 30 ± 5 nm. The lengths of the nanowires can be up to tens of micrometers. Parts a and b of Figure 4 are the TEM and high-resolution TEM images of a single Ga_2O_3 nanowire, respectively. The corresponding selected area electron diffraction (SAED) recorded along the [0−11] zone axis of the nanowire is also shown in the inset of Figure 4b, indicating the single-crystal nature of the synthesized β-Ga_2O_3 nanowires. By combining high-resolution TEM with defocused electron diffraction technique, the axis direction of Ga_2O_3 nanowires is determined to be along the [111] direction. Alternatively, from our extensive TEM examinations, the Ga_2O_3 nanowires terminating in a nanoparticle are frequently observed, as shown in Figure 4a, and the EDX analyses (data not shown here) show that the nanoparticles are Au-containing alloys (Au, Ga, O, and a slight amount of Si could be detected in the nanoparticles). This phenomenon indicates that the growth of the Ga_2O_3 nanowires follows the pattern of the vapor−liquid−solid (VLS) mechanism.[15]

In our experiments, the water vapor is introduced into the system and the following reaction may take place at the reaction temperature:

$$2Ga\ (l) + H_2O\ (g) \rightarrow Ga_2O\ (g) + H_2\ (g) \qquad (1)$$

$$Ga_2O\ (g) + 2H_2O\ (g) \rightarrow Ga_2O_3\ (s) + 2H_2\ (g) \qquad (2)$$

The reaction temperature of 900 °C is far lower than the boiling points of both metal Ga and Ga_2O_3; however, it is high enough to vaporize the Ga_2O.[16] The Ga_2O vapor reached to the surface of the substrate, and it and the transported water vapor were absorbed by Au nanoparticles formed by splitting a gold layer in the heating process.[17] Reaction 2 took place within the

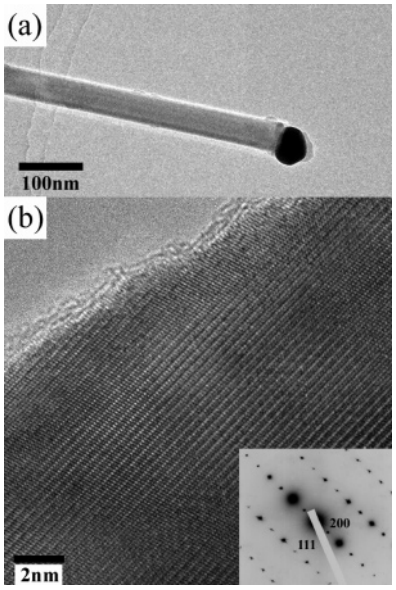

Figure 4. (a) Typical transmission electron microscope image of a Ga_2O_3 nanowire terminated by a nanoparticle; (b) high-resolution TEM images for the Ga_2O_3 nanowire and (inset) the corresponding selected area electron diffraction (SAED) pattern recorded along the [0−11] zone axis.

alloy droplets, and Ga_2O_3 nanowires began to grow following the VLS mechanism.

In our experiments, FIB-deposited Pt electrodes are first used to study the electrical properties of Ga_2O_3 nanowires because the focused ion-beam-assisted deposition technique is a fast and precise way to make electrodes, allowing ion-beam imaging of the individual nanowire and then in situ deposition of Pt as electrodes.[18,19] However, the measurement results show that the I−V curves (shown in Figure 5a) taken before and after annealing the device both exhibit nonlinear character and have higher slopes at high-bias voltages. Such behavior is typical for nanowire devices with Schottky barrier contacts on both sides.[20] The annealing process only slightly reduces the effect of the barrier between the Pt and Ga_2O_3 and leads to an increase of current, but it does not yield ohmic contacts, although that is necessary to study the intrinsic properties of semiconducting nanotubes or nanowires.[21]

In general, contact properties depend on the difference of work function between the electrodes and the semiconducting nanowires and also on the type of majority carriers. When the work function of the contact metal is larger than that of the semiconductor, an *n*-type semiconductor exhibits a Schottky barrier while a *p*-type semiconductor exhibits ohmic contact.[22] Because the work function of Pt is about 5.7 eV larger than that of Ga_2O_3 (about 5.0 eV), the conclusion that Sochottky barriers exist between the Ga_2O_3 nanowire and the Pt contacts implies that the as-grown Ga_2O_3 nanowire is an *n*-type semiconductor.

To obtain ohmic contact, the metal Ti with lower work function (4.33 eV) was used to make electrodes. Linear I−V curves were obtained, even when a slightly high-bias voltage was applied, indicating that ohmic contact was established between the Ti and Ga_2O_3. Figure 5b shows the SEM image of the contact device and the measured I−V curve. The distance between the two electrodes is 5 μm, and the diameter of the nanowire is approximately 40 nm; therefore, the conductivity of the individual nanowire can be estimated. Measurement of more than 10 individual nanowires in this method indicates that the as-grown β-Ga_2O_3 nanowires behave as typical semiconductors with good conductivity ($\sim 1\ \Omega^{-1}\cdot cm^{-1}$) in air. This value is about 11 orders of magnitude larger than the conductivity of the insulating Ga_2O_3 films deposited by electron-beam evaporation.[5,23] In our synthesis process, no dopant has been introduced in our sample, and the high conductivity of the Ga_2O_3 nanowires can be attributed to the enriched oxygen vacancies because the oxidizability of water vapor was weak and H_2 gas generated in reactions 1 and 2 possibly led to a reducing atmosphere. This is consistent with the previous studies.[5]

The gas-sensing measurements were also performed for an individual Ga_2O_3 nanowire device with two Au/Ti electrodes, and the source-drain biased voltage was fixed at 10 V. Figure 6 shows the electrical response of the Ga_2O_3 nanowires when the air-diluted NH_3 or NO_2 with different concentrations was flowing into the chamber. When the individual Ga_2O_3 nanowire was exposed to a mixed flow of ammonia (1000 ppm) and air, the current increased dramatically in the first 100 seconds, enhanced by more than 30 times. The current continued to increase, but slowly with increasing time, and was stable at $\sim$7800 nA. If the sensitivity S_g is defined as R_a/R_g, where R_a and R_g are the resistance before and after exposure, respectively, and the response time is defined as the time for the conductance to change by 1 order of magnitude, the individual Ga_2O_3 nanowire device exhibited a sensitivity of about 38 and a response time of $\sim$58 s in the ambient of 1000-ppm air-diluted

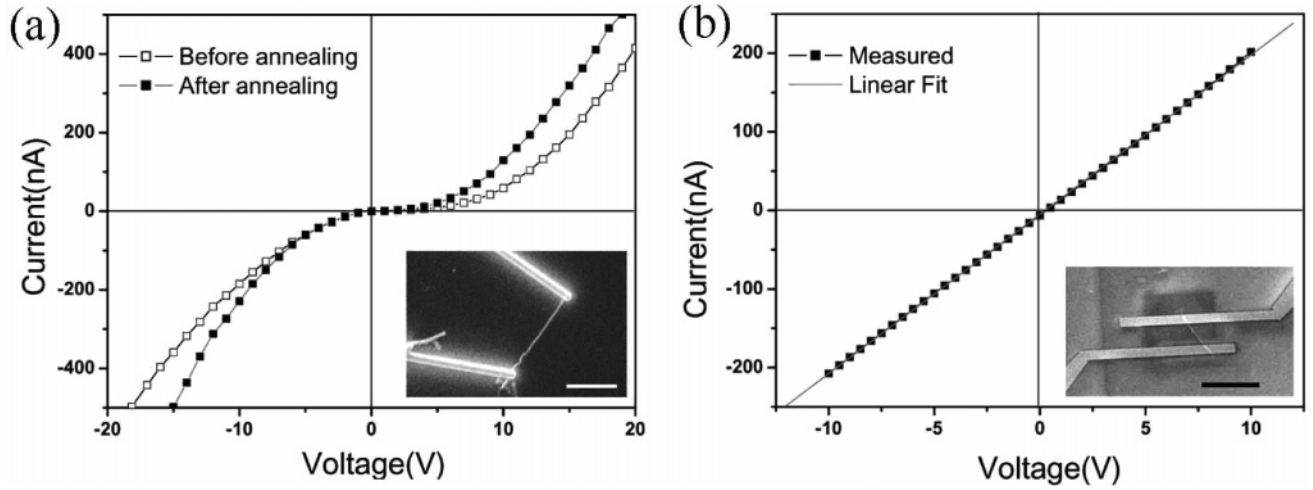

Figure 5. I−V curves obtained from individual Ga_2O_3 nanowire devices with (a) the Pt electrodes and (b) the Ti electrodes, respectively. Insets show the SEM images of the corresponding devices. Both of the scale bars in the insets are 5 μm.

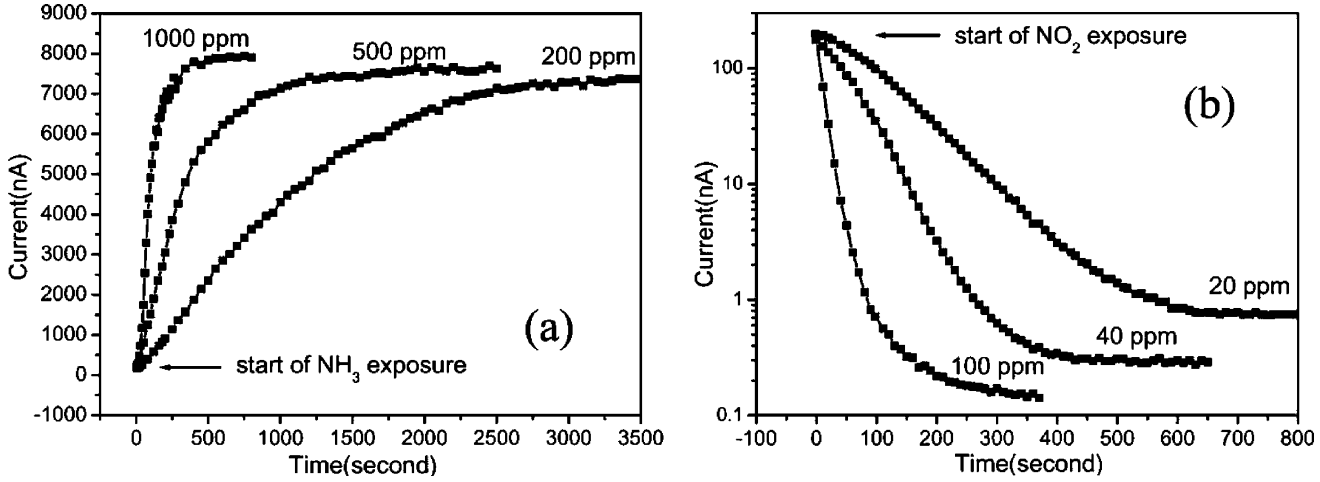

Figure 6. The current response of the individual Ga_2O_3 nanowires devices (a) to dry air-diluted NH_3 and (b) to air-diluted NO_2, respectively. The source-drain bias was fixed at 10 V.

NH_3. We have found that, after the exposure of the individual Ga_2O_3 nanowire device to the air-diluted NH_3 with different concentrations (from 1000 to 200 ppm), the current always increased and was eventually stable at a similar level, as shown in Figure 6a; however, the response time to NH_3 increased very quickly as the NH_3 concentrations decreased. The concentrations of 1000, 500, and 200 ppm relate to the response times of ~58 s, ~2 min, and ~6 min, respectively. In contrast, as shown in Figure 6b, when the air-diluted NO_2 flow (100 ppm) was introduced into the chamber, the current decreased by about 3 orders within 200 s, and finally stabilized at ~0.1 nA. The sensitivity (defined as R_g/R_a) and the response time is $\sim 1.2 \times 10^3$ and 28 s, respectively. The device exhibited a slightly lower sensitivity and longer response time when exposed to the air-diluted NO_2 with lower concentration. To 40 ppm NO_2, the sensitivity and the response time were $\sim 0.65 \times 10^3$ and ~125 s, respectively; to 20 ppm NO_2, the sensitivity and the response time were $\sim 0.25 \times 10^3$ and 240 s, respectively. This observation indicates that the conductivity of Ga_2O_3 nanowires is extremely sensitive to NH_3 and NO_2 at room temperature. This result is very interesting because previously reported Ga_2O_3 film sensors were usually operated at a high temperature (400−1000 °C) in order to achieve enhanced chemical reactivity between the sensitive materials and the surrounding gases. The room temperature sensitivity observed here is most likely to be due to the ultrahigh surface-to-volume ratios of the one-dimensional nanostructures, which is very beneficial to the adsorption of gas molecules on the surface. The conductivity of the Ga_2O_3 is very sensitive to the nature and concentration of adsorbed species on its surface. The adsorption of reducing NH_3 molecules, which tend to lose electrons, is likely to increase the carrier concentration in the *n*-type Ga_2O_3 nanowires and lead to greatly enhanced conductivity. In contrast, the adsorption of oxidizing NO_2 molecules on the surface of the Ga_2O_3 nanowires is likely to trap electrons and reduce the conductivity of nanowires. In fact, we have found that some other gases, such as H_2S and SO_2, with characteristics similar to NH_3 or NO_2, could also intensively influence the conductivity of an individual Ga_2O_3 nanowire.

4. Conclusion

In summary, we proposed a novel method to prepare highly crystallized β-Ga_2O_3 nanowires with a high aspect ratio by reacting metal Ga with water vapor. Both the SEM and the TEM examinations indicate that Ga_2O_3 nanowires grow within the vapor−liquid−solid growth mechanism. Study of the electrical properties of an individual Ga_2O_3 nanowire indicates that Ti can form ohmic contacts with the Ga_2O_3 nanowires, while Pt forms Schottky-barrier junctions. The conductivity of *n*-type semiconducting Ga_2O_3 nanowires is extremely sensitive to NH_3 or NO_2, even at room temperature. In air, the Ga_2O_3 nanowires have a conductivity of $\sim 1\ \Omega^{-1}\cdot cm^{-1}$, while with adsorption of the NH_3 (or NO_2) molecules, the conductivity can increase (or decrease) by more than 30 times (or 2 orders).

Acknowledgment. This work was supported by the State Key Development Program for Basic Research of China (grant no. 2002CB613500), Outstanding Youth Foundation of Hubei Province, Fok Ying Tong Education Foundation (grant no. 91059), and the National Center for Nanoscience and Technology, China.

References and Notes

(1) Dai, H.; Wong, E. W.; Lu, Y. Z.; Fan S.; Lieber C. M. *Nature* **1995**, *375*, 769.

(2) Wang, D. W.; Wang, Q.; Javey, A.; Tu, R.; Dai, H. J.; Kim, H.; McIntyre, P. C.; Krishnamohan, T.; Saraswat, K. C. *Appl. Phys. Lett.* **2003**, *83*, 2432.

(3) Arnold, M. S.; Avouris, P.; Pan, Z. W.; Wang, Z. L. *J. Phys. Chem. B* **2003**, *107*, 659.

(4) Li, C.; Zhang, D.; Liu, X.; Han, S.; Tang, T.; Han, J.; Zhou, C. *Appl. Phys. Lett.* **2003**, *82*, 1613.

(5) Lorenz, M. R.; Woods, J. F.; Gambino, R. J. *J. Phys. Chem. Solids* **1967**, *28*, 403.

(6) Binet, L.; Gourier, D. *J. Phys. Chem. Solids* **1998**, *59*, 1241.

(7) Li, Z.; Groot, C. D.; Moodera, J. H. *Appl. Phys. Lett.* **2000**, *77*, 3630.

(8) Ogita, M.; Higo, K.; Nakanishi, Y.; Hatanaka, Y. *Appl. Surf. Sci.* **2001**, *175*, 721.

(9) Zhang, H. Z.; Kong, Y. C.; Wang, Y. Z.; Du, X.; Bai, Z. G.; Wang, J. J.; Yu, D. P.; Ding, Y.; Hang, Q. L.; Feng, S. Q. *Solid State Commun.* **1999**, *109*, 677.

(10) Tang, C. C.; Fan, S. S.; Lamy de la Chapelle, M.; Li, P. *Chem. Phys. Lett.* **2001**, *333*, 12.

(11) Hu, J. Q.; Li, Q.; Meng, X. M.; Lee, C. S.; Lee, S. T. *J. Phys. Chem. B* **2002**, *106*, 9536.

(12) Wu, X. C.; Song, W. H.; Huang, W. D.; Pu, M. H.; Zhao, B.; Sun, Y. P.; Du, J. J. *Chem. Phys. Lett.* **2000**, *328*, 5.

(13) Fu, L.; Liu, Y.; Hu, P.; Xiao, K.; Yu, G.; Zhu, D. *Chem. Mater.* **2003**, *15*, 4287.

(14) Valcárcel, V.; Souto, A.; Guitián, F. *Adv. Mater.* **1998**, *10*, 138.

(15) Wu, Y.; Yang, P. *J. Am. Chem. Soc.* **2001**, *123*, 3165.

(16) Greenwood, N. N.; Earnshaw, A. *Chemistry of the Elements*, 2nd ed.; Butterworth: London, 1997.

(17) Huang, M. H.; Wu, Y.; Feick, H.; Tran, N.; Weber, E.; Yang, P. *Adv. Mater.* **2001**, *13*, 113.
(18) Lin, J.-F.; Bird, J. P.; Rotkina, L.; Bennett, P. A. *Appl. Phys. Lett.* **2003**, *82*, 802.
(19) Long, Y.; Chen, Z.; Wang, W.; Bai, F.; Jin, A.; Gu, C. *Appl. Phys. Lett.* **2005**, *86*, 153102.
(20) Chung, S.; Yu J.; Heath, J. R. *Appl. Phys. Lett.* **2000**, *76*, 2068.
(21) Bezryadin, A.; Verschueren, A. R.; M. Tans, S. J.; Dekker, C. *Phys. Rev. Lett.* **1998**, *80*, 4036.
(22) Wang, D.; Lua, J. G.; Otten, C. J.; Buhro, W. E. *Appl. Phys. Lett.* **2003**, *83*, 5280.
(23) Passlack, M.; Hunt, N. E. J.; Schubert, E. F.; Zydzik, G. J.; Hong, M.; Mannaerts, J. P.; Opila, R. L.; Fischer R. J. *Appl. Phys. Lett.* **1994**, *64*, 2715.